Research Article | Open Access

Chemical Synthesis

Wang *et al. Chem. Synth.* **2026**, *6*, 56 **DOI:**10.20517/cs.2026.01

Solvothermal synthesis and formation mechanism of lithium dodecaborate

Jian Wang[1,2], Timothy Steenhaut[1], Koen Robeyns[1], Hai-Wen Li[2,*], Yaroslav Filinchuk[1,*]

Keywords:
Metal dodecaborate, $Li_2B_{12}H_{12}$, undecaborates, reaction mechanism, boron chemistry

Citation: Wang, J.; Steenhaut, T.; Robeyns, K.; Li, H. W.; Filinchuk, Y. Solvothermal synthesis and formation mechanism of lithium dodecaborate. *Chem. Synth.* **2026**, *6*, 56. https://dx.doi.org/10.20517/cs.2026.01

Received: 2 Jan 2026
First Decision: 21 Jan 2026
Revised: 26 Jan 2026
Accepted: 2 Feb 2026
Published: 17 Jun 2026

Academic Editor:
Xiaoxin Zou
Copy Editor:
Pei-Yun Wang
Production Editor:
Pei-Yun Wang

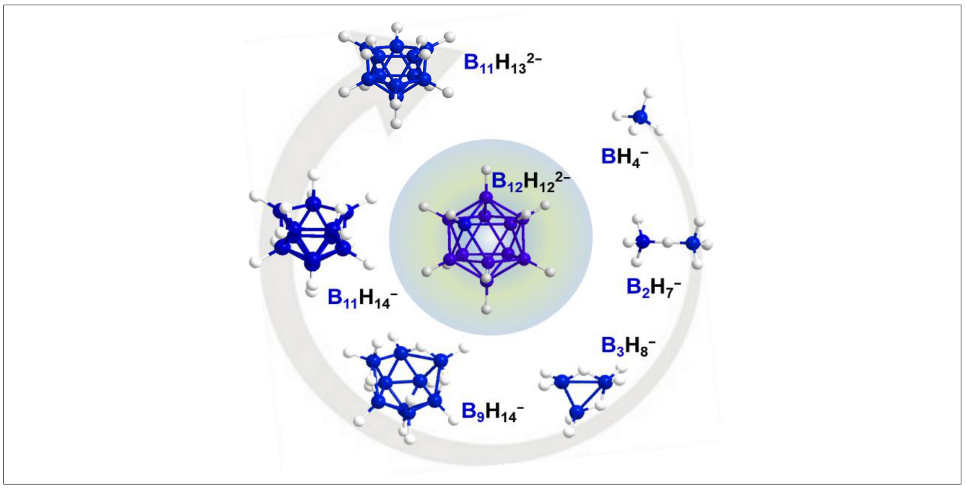

Abstract

Metal dodecaborates, particularly lithium dodecaborate ($Li_2B_{12}H_{12}$), are promising ionic conductors, but their broader application is hindered by complex synthesis. Here, we report a facile solvothermal synthesis of $Li_2B_{12}H_{12}$ via the reaction of lithium borohydride ($LiBH_4$) with borane dimethyl sulfide complex ($DMS{\cdot}BH_3$) in glyme solvents. This synthesis can be conveniently performed either in a Schlenk flask (with or without reflux) or in an autoclave, demonstrating high yields (up to 96%) and excellent purity. The enclosed system provided by the autoclave was shown to be more favorable for the synthesis of the $B_{12}H_{12}^{2-}$ anion. A detailed mechanistic investigation utilizing ^{11}B nuclear magnetic resonance (^{11}B NMR) spectroscopy revealed the stepwise formation of $B_2H_7^-$, $B_3H_8^-$, $B_9H_{14}^-$, $B_{11}H_{14}^-$, and $B_{11}H_{13}^{2-}$ intermediates. This synthetic strategy was successfully extended to other alkali metal dodecaborates (Na, K), and their glyme-coordinated complexes were characterized by single-crystal X-ray diffraction. Furthermore, we introduce a solvent-exchange approach using weakly coordinating solvents such as dimethyl sulfoxide (DMSO) or water, enabling simple and efficient desolvation, thereby offering a practical new approach to obtain anhydrous metal dodecaborates.

Check for updates

[1]Institute of Condensed Matter and Nanosciences, Université catholique de Louvain, Louvain-la-Neuve 1348, Belgium.
[2]School of Advanced Energy, Sun Yat-sen University, Shenzhen 518107, Guangdong, China.

***Correspondence to:** Prof. Hai-Wen Li, School of Advanced Energy, Sun Yat-sen University, Shenzhen 518107, Guangdong, China. E-mail: lihw76@mail.sysu.edu.cn; Prof. Yaroslav Filinchuk, Institute of Condensed Matter and Nanosciences, Université catholique de Louvain, Louvain-la-Neuve 1348, Belgium. E-mail: yaroslav.filinchuk@uclouvain.be

INTRODUCTION

The dodecahydro-*closo*-dodecaborate anion ($B_{12}H_{12}^{2-}$) has emerged as a versatile building block in advanced energy materials owing to its unique combination of properties[1-7]. This icosahedral cluster (theoretically predicted in the 1950s and first isolated in 1960) exhibits exceptional thermal and chemical stability and a highly delocalized charge, leading to the high ionic conductivity of its metal salts and enabling structural tunability through substitutions[8-14]. These properties have contributed to its increasing importance in a wide range of applications, notably as a superionic charge carrier in solid-state electrolytes, where recent studies have demonstrated fast lithium (Li)-ion transport, wide electrochemical stability windows, and improved safety compared to conventional liquid electrolytes[12,15-22], and as a boron-rich, water-soluble, and biocompatible agent with potential applications in high-energy materials, boron neutron capture therapy (BNCT), and various other functional systems[23-27]. However, the broader implementation of $B_{12}H_{12}^{2-}$ is impeded by the lack of simple and scalable synthetic routes, which remains a major constraint on its broader application[3,4,11,28].

Conventional synthetic routes for $B_{12}H_{12}^{2-}$ salts generally rely on either multi-step wet-chemical synthesis combined with ion exchange processes or solvent-free methods, as illustrated in Figure 1. In the classical solution-based route [Figure 1A], volatile borane precursors (e.g., B_2H_6, $B_{10}H_{14}$) react with borohydride anions in a high-boiling-point ethereal solvent[29]. To remove the strongly coordinating solvents, a widely adopted strategy involves an ion exchange step using amine complexes with bulky cations, typically yielding $[(C_2H_5)_3NH]_2B_{12}H_{12}$ as a water-insoluble intermediate. Subsequent ion exchange of this compound with metal hydroxides (or hydrides) allows for the preparation of the desired metal $B_{12}H_{12}$. Although this method yields hydrated metal dodecaborates and has been the preferred choice in earlier studies, its main drawbacks are operational complexity and high cost[30-32]. Solvent-free approaches [Figure 1B], based on ball milling or annealing, have gained popularity in recent years due to their ability to produce anhydrous $B_{12}H_{12}^{2-}$ salts in a single step[33-35]. However, these approaches often result in the co-formation of other boron-rich compounds. In addition, both methods present concerns regarding product yield and purity, as well as the toxicity and reactivity of the specific borane precursors, which continue to pose significant challenges.

Incremental improvements in synthetic approaches toward $B_{12}H_{12}^{2-}$ have mainly focused on replacing diborane with reducing agents that present fewer handling issues[36-39]. With this in mind, we recently achieved the synthesis of unsolvated sodium and potassium dodecaborates ($Na_2B_{12}H_{12}$ and $K_2B_{12}H_{12}$) by reacting the borane dimethyl sulfide complex ($DMS{\cdot}BH_3$) with the corresponding borohydride ($NaBH_4$ or KBH_4) in diglyme under heating in an autoclave. The use of diglyme was found to facilitate the removal of all intermediate products formed during the reaction, leading to high-purity $M_2B_{12}H_{12}$ (M = Na or K)[36]. Lithium dodecaborate ($Li_2B_{12}H_{12}$) has recently attracted attention as an important precursor for producing Li-ion solid-state electrolytes[15-18,40]. In contrast to its sodium and potassium counterparts, limited research has been conducted on direct solution-phase synthetic approaches for obtaining this compound. Furthermore, due to the strong tendency of Li^+ to coordinate with the ethereal solvents used in the synthesis, the production of unsolvated $Li_2B_{12}H_{12}$ is particularly challenging[41,42]. One alternative approach involves exchanging Li^+ with large monovalent cations, such as trimethylammonium, to yield water-insoluble products and enable the removal of diglyme [Figure 1A]. Anhydrous $Li_2B_{12}H_{12}$ can then be obtained through a second cation substitution in the resulting $[(C_2H_5)_3NH]_2B_{12}H_{12}$ using LiOH in water, followed by heat treatment to readily remove the water[43]. However, this approach involves several steps and can introduce impurities if the amount of LiOH is not carefully controlled. In addition to the synthesis of $B_{12}H_{12}^{2-}$, cation exchange has been widely employed in the preparation of various metal borate compounds, including $B_{11}H_{14}^-$, $CB_{11}H_{12}^-$, and other metal borates[15,37,41,44]. These methods typically yield hydrated metal borates as intermediates, from which water can be removed under mild conditions to obtain the corresponding unsolvated salts. Such

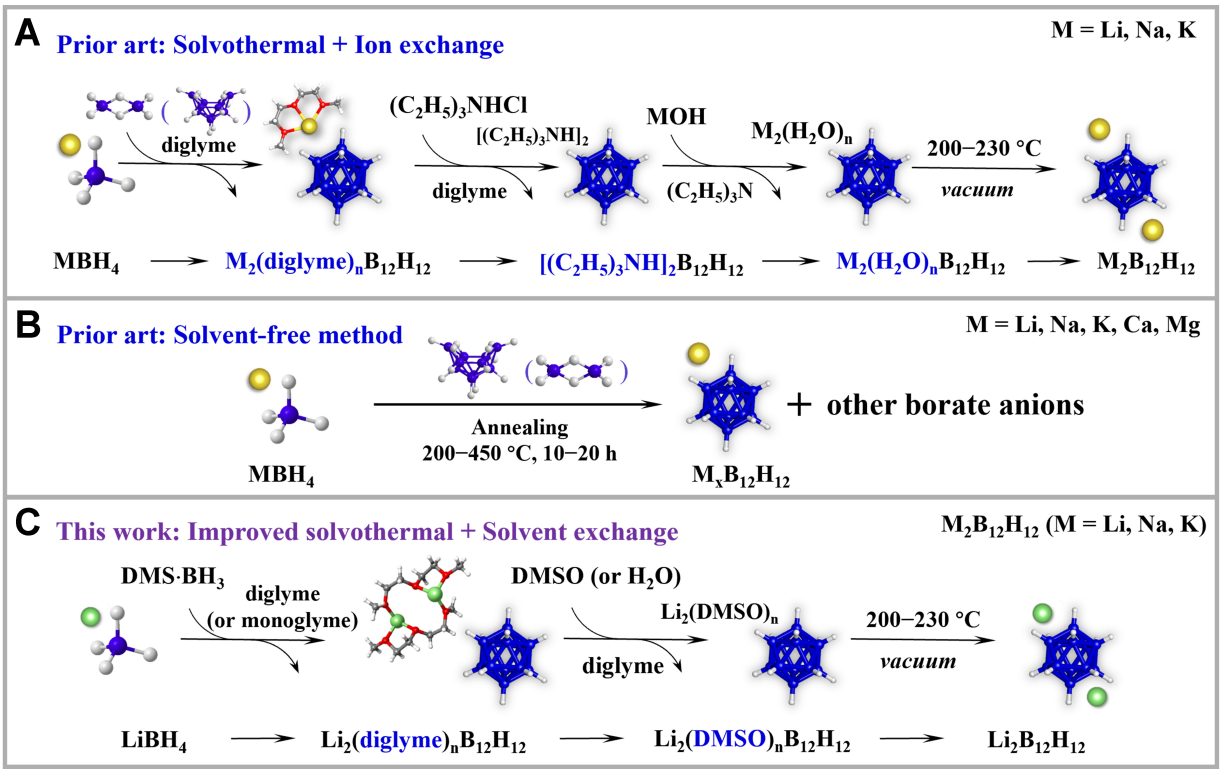

Figure 1. Comparative synthetic strategies for the preparation of metal dodecaborates. (A) Conventional solution-based synthesis followed by multi-step cation exchange; (B) Solvent-free synthesis; (C) This works: improved solvothermal synthesis followed by a solvent-exchange step. DMS·BH_3: Borane dimethyl sulfide complex; DMSO: dimethyl sulfoxide; $LiBH_4$: lithium borohydride; $Li_2B_{12}H_{12}$: lithium dodecaborate.

approaches often require multiple ion exchange steps and strict control of the exchange conditions. Therefore, a more straightforward and general strategy that avoids these complications would be highly desirable.

Since the observation of $B_{12}H_{12}^{2-}$ formation as a "boron sink" during the dehydrogenation of BH_4^-, extensive experimental and computational work has been carried out to demystify the conversion process leading to $B_{12}H_{12}^{2-}$[34,37,45-49]. These studies demonstrated that BH_4^- can undergo a variety of pathways to form higher monovalent anions such as $B_3H_8^-$, $B_9H_{14}^-$, and $B_{11}H_{14}^-$. The stepwise formation of larger polyhedral boranes from smaller boron clusters can be described as a series of reactions involving the incorporation of neutral boron hydrides, such as B_2H_6, into the BH_4^- anion. Indeed, small charged boron species, such as BH_4^- and $B_3H_8^-$, tend to react with strongly electrophilic neutral boron hydrides, including L·BH_3 (L = Lewis base), B_2H_6, B_4H_{10}, and $B_{10}H_{14}$, owing to their nucleophilicity[45,50,51]. However, the formation mechanism of the final dianion ($B_{12}H_{12}^{2-}$) from monovalent anions and neutral boron hydrides has not yet been well understood.

In this contribution, we present a novel and convenient synthetic approach [Figure 1C] for the preparation of highly pure anhydrous alkali metal dodecaborates, including $Li_2B_{12}H_{12}$. The first step is based on reacting lithium borohydride ($LiBH_4$) with DMS·BH_3 in a heated solvent using either conventional Schlenk techniques [Supplementary Figures 1-3] or an autoclave. In the second step, a solvent exchange strategy coupled with thermal treatment is used to desolvate the product. Finally, the formation mechanism of $B_{12}H_{12}^{2-}$ is experimentally investigated by solution-state ^{11}B nuclear magnetic resonance (^{11}B NMR) spectroscopy.

EXPERIMENTAL

Synthesis of $Li_2B_{12}H_{12}$ in a Schlenk flask

Typically, 0.11 g of $LiBH_4$ (5 mmol, 95%) was weighed into a glass frit-equipped Schlenk flask within a glovebox, and the flask was then sealed with a rubber septum before being removed from the glovebox. Subsequently, 20 mL of diglyme and 27.5 mmol (2.75 mL) of $(CH_3)_2S{\cdot}BH_3$ were added outside the glovebox using standard Schlenk techniques [Supplementary Figure 2A]. The solution was then heated to 120 °C, and the initially colorless solution turned yellow after approximately 2 h, accompanied by the formation of a white precipitate. The reaction mixture was further stirred at 120 °C for 24 h. The reaction solution was allowed to cool naturally to room temperature and was then filtered (using a 10-16 μm fritted glass filter) and washed with diglyme (3 × 5 mL). The resulting sample was dried under vacuum at 80 °C for 2 h to remove residual solvent. The solvated product, $Li_2B_{12}H_{12}{\cdot}n\ C_6H_{13}O_3$, was obtained as a white crystalline solid with a yield of approximately 40% $Li_2B_{12}H_{12}$ based on the amount of $LiBH_4$ used.

Synthesis of $Li_2B_{12}H_{12}{\cdot}n$ diglyme in an autoclave

Typically, 0.11 g of $LiBH_4$ (5 mmol) was weighed into a quartz-lined reactor inside a glovebox and sealed with Parafilm®. Immediately before loading the quartz reactor into the autoclave, 20 mL of diglyme followed by 27.5 mmol (2.75 mL) of $(CH_3)_2S{\cdot}BH_3$ were quickly added to the borohydride. The autoclave was then sealed and purged with argon for 30 s to remove air from the system. The reaction temperature was increased from room temperature to 120 °C at a rate of 2 °C/min and maintained at this temperature for 24 h. After the system had cooled to room temperature, the reaction mixture was filtered using a Schlenk filtration apparatus [Supplementary Figure 2A] and washed with diglyme (3 × 5 mL). The sample was finally dried under vacuum at 80 °C for 2 h. The yield of $Li_2B_{12}H_{12}$ was approximately 91%, based on the amount of $LiBH_4$ used.

Synthesis of $Li_2B_{12}H_{12}{\cdot}n$ DME in an autoclave

Typically, 0.22 g of $LiBH_4$ (10 mmol) was weighed into a quartz-lined reactor inside a glovebox and sealed with Parafilm®. Immediately before loading the quartz reactor into the autoclave, 20 mL of monoglyme followed by 55 mmol (5.5 mL) of $(CH_3)_2S{\cdot}BH_3$ were quickly added to the borohydride. The autoclave was then sealed and purged with argon for 30 s to remove air from the system. The reaction temperature was increased from room temperature to 120 °C at a rate of 2 °C/min and maintained at this temperature for 24 h. After the system had cooled to room temperature, the reaction mixture was transferred into a Schlenk flask equipped with a filtration glass frit [Supplementary Figure 2A] and cooled in a refrigerator overnight (10 °C). At this stage, part of the product crystallized from the solution. The sample was then washed with cold monoglyme (10 °C, 3 × 10 mL) under an inert atmosphere, and finally dried under vacuum at room temperature for 2 h. The resulting $Li_2B_{12}H_{12}{\cdot}n$ DME (DME, 1,2-dimethoxyethane) was obtained with an approximately 89% yield of $Li_2B_{12}H_{12}$ based on the amount of $LiBH_4$ used.

Solvent exchange of $Li_2B_{12}H_{12}{\cdot}n$ diglyme with DMSO

Typically, 1 g of dried $Li_2B_{12}H_{12}{\cdot}n$ diglyme was suspended in 10 mL of dimethyl sulfoxide (DMSO) in a glass frit-equipped Schlenk flask. Subsequently, the suspension was heated at 100 °C under vacuum to remove residual volatile solvents, affording $Li_2B_{12}H_{12}{\cdot}n$ DMSO as a solid product. Final desolvation was achieved by thermal treatment at 200 °C for 12 h under dynamic vacuum, affording anhydrous $Li_2B_{12}H_{12}$ as a white crystalline solid.

Solvent exchange of $Li_2B_{12}H_{12}{\cdot}n$ DME with H_2O

Typically, 1 g of dried $Li_2B_{12}H_{12}{\cdot}n$ DME was suspended in 10 mL of deionized water in a glass frit-equipped Schlenk flask. Subsequently, the suspension was heated at 40 °C under vacuum to remove residual solvents,

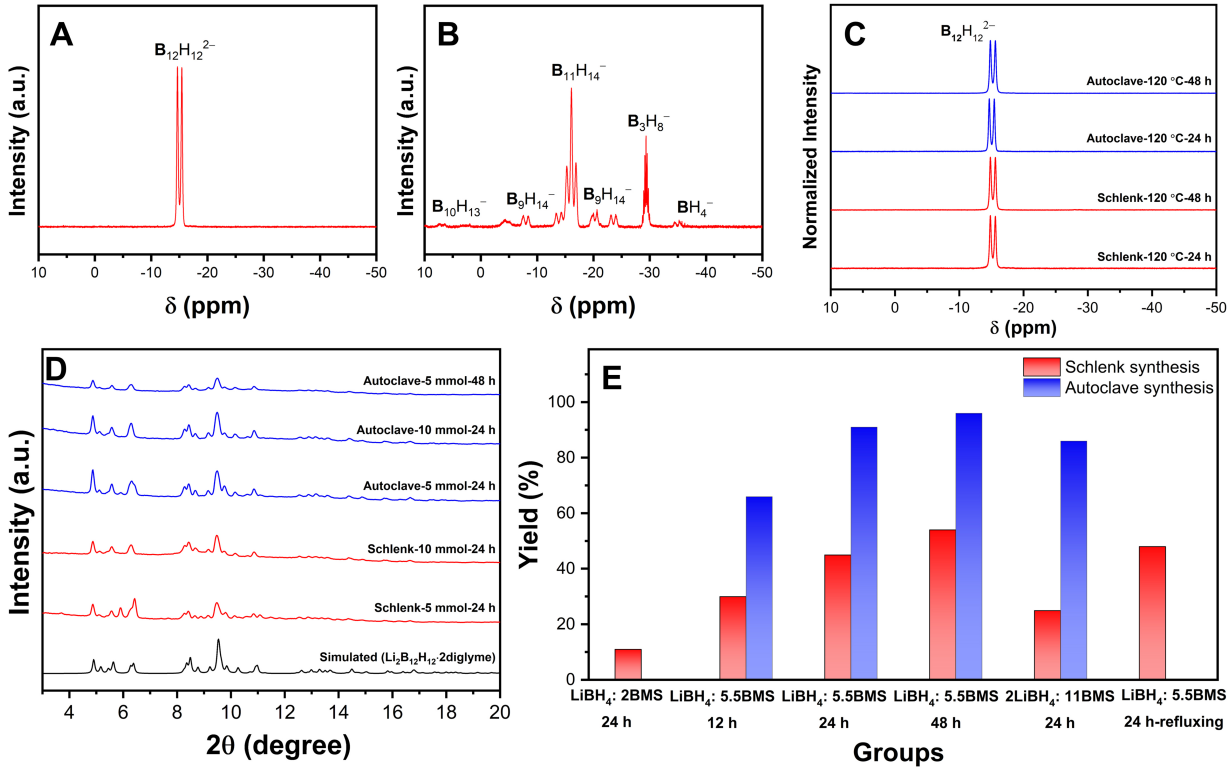

Figure 2. Proton-coupled ^{11}B NMR spectra of reaction products: (A) solid precipitate and (B) filtrate after 24 h reaction at 120 °C in a Schlenk setup (5 mmol $LiBH_4$ + 27.5 mmol DMS·BH_3); (C) PXRD patterns of selected as-synthesized $Li_2B_{12}H_{12}$·n diglyme samples (λ = 0.71073 Å); (D) Proton-coupled ^{11}B NMR spectra of selected as-synthesized $Li_2B_{12}H_{12}$·n diglyme samples; (E) Yields of selected as-synthesized $Li_2B_{12}H_{12}$·n diglyme samples. ^{11}B NMR: ^{11}B nuclear magnetic resonance; $LiBH_4$: lithium borohydride; DMS·BH_3: borane dimethyl sulfide complex; PXRD: powder X-ray diffraction; $Li_2B_{12}H_{12}$: lithium dodecaborate.

affording $Li_2B_{12}H_{12}$·n H_2O as a solid product. Final desolvation was achieved by thermal treatment at 200 °C for 12 h under dynamic vacuum, affording anhydrous $Li_2B_{12}H_{12}$ as a white crystalline solid.

More experimental details are available in the Supplementary Materials.

RESULTS AND DISCUSSION

Synthesis of $Li_2B_{12}H_{12}$ and its optimization

In the first step of our new synthetic method, $LiBH_4$ is reacted with DMS·BH_3 in diglyme to produce $Li_2B_{12}H_{12}$, following Equation (1). This reaction was first investigated using a classical Schlenk setup at 120 °C with a molar ratio of 1:5.5 (10% excess DMS·BH_3) [Supplementary Figure 4].

$$2MBH_4 + 10(CH_3)_2S \cdot BH_3 \xrightarrow{diglyme} M_2B_{12}H_{12} \cdot nC_6H_{14}O_3 + 10(CH_3)_2S + 13H_2 \ (M = Li, Na, K) \quad (1)$$

After 24 h, the yield of $B_{12}H_{12}^{2-}$ in the solid product reached 45%, as shown by the sole presence of a doublet at around -15.2 ppm in the proton-coupled ^{11}B solution-state NMR spectrum of the solid product dissolved in DMSO-d_6 [Figure 2A][31,52,53]. NMR analysis of the filtrate [Figure 2B] revealed residual intermediates such as $B_3H_8^-$ and higher-nuclearity boron clusters, including $B_9H_{14}^-$, $B_{10}H_{13}^-$, and $B_{11}H_{14}^-$, all of which are soluble in diglyme[42,54-56].

To optimize the reaction conditions, the DMS·BH_3 ratio was varied while maintaining all other parameters constant (5 mmol $LiBH_4$, 20 mL diglyme, and 24 h of heating at 120 °C). Experiments were carried out with $LiBH_4$/DMS·BH_3 molar ratios of 1:2 and 1:10. The 1:2 ratio, which is optimal for the synthesis of $B_3H_8^-$,

resulted in a $Li_2B_{12}H_{12}$ yield of approximately 11% based on the amount of $LiBH_4$ used, with $B_3H_8^-$ remaining as the main boron species in the filtrate [Supplementary Figures 4 and 5, Supplementary Table 2]. In contrast, the 1:10 ratio yielded 25% $Li_2B_{12}H_{12}$ and produced $B_{11}H_{14}^-$ as the main boron species in the filtrate. Excess DMS·BH_3 thus slightly increases $Li_2B_{12}H_{12}$ yield but reduces BH_3 utilization efficiency due to the formation of higher-nuclearity boron clusters ($B_9H_{14}^-$, $B_{11}H_{14}^-$), which deplete BH_3 in the reaction mixture[55].

Temperature is a crucial factor in the synthesis of polyhedral borates, and its influence was therefore also investigated in this work[36,37]. At a lower temperature (85 °C), incomplete conversion of BH_4^- and DMS·BH_3 into $B_3H_8^-$, $B_9H_{14}^-$, $B_{10}H_{13}^-$, and $B_{11}H_{14}^-$ was observed after 24 h, as shown by ^{11}B NMR [Supplementary Figure 6], leading to a yellow reaction solution without precipitation. After extending the reaction time to 48 h, a very small amount of precipitate appeared, and the ^{11}B NMR spectrum [Supplementary Figure 6] showed weak signals of $B_{12}H_{12}^{2-}$ and near-complete depletion of $LiBH_4$. At a higher temperature (160 °C) without a condenser, a poly-anionic species formed directly [Supplementary Figure 7]. We speculate that this species might arise from a reaction between $B_{11}H_{14}^-$ and partially dehydrogenated $B_{12}H_{12-x}^{2-}$ anions. Dehydrogenation of the icosahedral $B_{12}H_{12}^{2-}$ cluster alters the charge and symmetry of the twelve BH vertices, leading to the formation of disubstituted anions when reacted with electrophilic compounds[57]. Performing the same experiment at 160 °C but using a setup equipped with a condenser resulted in the formation of $B_{12}H_{12}^{2-}$, along with some $B_{10}H_{10}^{2-}$ and partially dehydrogenated $B_{12}H_{12-x}^{2-}$ anions [Supplementary Figure 8][58]. The use of a condenser also increased the yield compared to the reaction at 120 °C, as indicated in Supplementary Table 3. Additionally, the predominance of $B_{11}H_{14}^-$ in the filtrate [Supplementary Figure 9] indicates that refluxing promotes the conversion of lower boranes to $B_{12}H_{12}^{2-}$.

Similar reactions at 160 °C in Schlenk flasks equipped with a condenser [Supplementary Figure 10 and Supplementary Table 4], where $LiBH_4$ was substituted by $NaBH_4$ and KBH_4, produced $Na_2B_{12}H_{12}$ and $K_2B_{12}H_{12}$ in isolated yields of 92% and 88%, respectively. In this case, higher temperature favors the formation of $B_{12}H_{12}^{2-}$, which is in line with previous research showing that the thermal decomposition of BH_4^- and $B_3H_8^-$ salts can generate *closo*-borates such as $B_{10}H_{10}^{2-}$ and $B_{12}H_{12}^{2-}$[59-62]. Furthermore, in contrast to diglyme solvated $Li_2B_{12}H_{12}$, the solvates of $Na_2B_{12}H_{12}$ and $K_2B_{12}H_{12}$ are much more stable at this temperature[36]. The small amounts of $B_{10}H_{10}^{2-}$ impurities in $Na_2B_{12}H_{12}$ and $K_2B_{12}H_{12}$ can be completely removed by washing with diglyme. These results indicate that a Schlenk setup equipped with a condenser is suitable for high-yield synthesis of $Na_2B_{12}H_{12}$ and $K_2B_{12}H_{12}$ but is not ideal for $Li_2B_{12}H_{12}$ preparation.

Further optimization of the synthesis conditions was performed by varying the concentrations of reactants and reaction times. The resulting products consistently exhibited high purity under all tested conditions, as shown in Figure 2C and D. The reactions were performed either in a Schlenk setup without a condenser or in an autoclave, as the latter enables all generated gaseous species, such as B_2H_6 and DMS, to remain confined within the reaction volume. As a general trend, the yields of $Li_2B_{12}H_{12}$ obtained in the autoclave were much higher than those in the Schlenk setup. Based on the yield comparison presented in Figure 2E and Table 1, we speculate that B_2H_6 present in the autoclave atmosphere promotes the hydroboration reaction from BH_4^- to $B_{11}H_{14}^-$, thus improving the yield of $B_{12}H_{12}^{2-}$[31,37,38,42,50,60,63]. Detailed reaction conditions are summarized in Supplementary Tables 3-7 and Supplementary Figures 11 and 12. In addition, longer reaction times enabled complete conversion of the reactants, resulting in higher yields. Remarkably, an isolated yield of 96% pure $Li_2B_{12}H_{12}$ was achieved in the autoclave, representing, to the best of our knowledge, the highest yield achieved thus far for the preparation of metal dodecaborates [Supplementary Table 8]. When the reactant concentration in the autoclave was increased, a drop in yield was observed. This contrasts with the reactions in the Schlenk setup, for which increasing reactant concentrations or reaction times had no significant impact on the final yield of $B_{12}H_{12}^{2-}$.

Table 1. Screening of synthetic conditions for $Li_2B_{12}H_{12}$

Entry (*)	Reaction setup	Reagents		Reaction conditions		Yield of $Li_2B_{12}H_{12}$ (%)
		$LiBH_4$ (mmol)	$DMS{\cdot}BH_3$ (mmol)	Temperature (°C)	Time (h)	
1		5	10	120	24	11
2	Schlenk	5	27.5	120	12	30
	Autoclave					66
3	Schlenk	5	27.5	120	24	45
	Autoclave					91
4	Schlenk	5	27.5	120	48	54
	Autoclave					96
5	Schlenk	10	55	120	24	40
	Autoclave					86
6		5	27.5	120 (Refluxing)	24	48

$Li_2B_{12}H_{12}$: Lithium dodecaborate; $LiBH_4$: lithium borohydride; $DMS{\cdot}BH_3$: borane dimethyl sulfide complex.

Signals of $B_{10}H_{13}^-$ were not observed in the ^{11}B NMR spectra [Supplementary Figure 13] of filtrates resulting from autoclave experiments. The autoclave keeps all gaseous species under high pressure within the reactor system, and the B_2H_6 dimer can thus be retained in the reaction mixture. We speculate that the pyrolysis of B_2H_6 directly leads to the formation of higher boranes, such as B_4H_{10} or B_6H_{10}, resulting in an increased content of $B_{11}H_{14}^-$ in solution and a slow reaction between $B_3H_8^-$ and $B_{11}H_{14}^-$[64,65]. Remaining $DMS{\cdot}BH_3$ can be observed in the NMR spectra of products obtained from the autoclave system but not in those from reactions performed in a Schlenk flask.

The synthesis of $Li_2B_{12}H_{12}$ in an autoclave can also be carried out using a lighter ether such as monoglyme (DME, boiling point of 85 °C) as the solvent. Supplementary Figures 14 and 15 show the ^{11}B NMR spectra of the solid precipitate and filtrate obtained from the reaction of 10 mmol $LiBH_4$ with 55 mmol $DMS{\cdot}BH_3$ in 20 mL monoglyme. The ^{11}B NMR spectra [Supplementary Figures 14 and 15] demonstrate that under these conditions, pure $B_{12}H_{12}^{2-}$ is obtained, with an isolated yield of 42%. However, a considerable amount of $Li_2B_{12}H_{12}$ remains as small particles in the filtrate [Supplementary Figure 14B], which makes full recovery of the solid product difficult. Cooling the reaction solution in a refrigerator at 10 °C overnight before filtration addresses this issue by increasing crystallite size. By doing so, and washing the product with cold monoglyme (10 °C), a monoglyme-rich solvated $Li_2B_{12}H_{12}$ was obtained with an isolated yield of 89%.

Thermal behavior and desolvation of as-synthesized $M_2B_{12}H_{12}$

After initial drying, the crude products contained variable amounts of diglyme molecules per formula unit, as evidenced by NMR spectroscopy [Supplementary Figures 11 and 12]. Attempts to remove coordinated solvent from $Li_2B_{12}H_{12}{\cdot}$n diglyme by thermal treatment were unsuccessful. Thermogravimetric analysis (TGA) was performed to investigate the thermal stability and composition of the $Li_2B_{12}H_{12}{\cdot}$n diglyme adducts [Supplementary Figure 16]. The thermal decomposition proceeds in three steps: the removal of free diglyme starts at 25 °C (-9.5 wt.%), followed by a larger mass loss of 15.5 wt.% starting at around 150 °C and a third mass loss of 5 wt.% between 200 and 300 °C. The latter two steps are attributed to the removal of coordinated diglyme.

An *in situ* synchrotron radiation powder X-ray diffraction (SR-PXRD) experiment was performed to further investigate the behavior of $Li_2B_{12}H_{12}{\cdot}$n diglyme during thermal treatment [Supplementary Figure 17]. The only crystalline phase observed in the diffraction patterns corresponds to $Li_2B_{12}H_{12}{\cdot}$2 diglyme, which is

thermally stable up to 179 °C and then decomposes into an amorphous phase. The structure of $Li_2B_{12}H_{12}$·2 diglyme was determined by single crystal X-ray diffraction (SC-XRD; Figure 3A, Supplementary Figure 59, Supplementary Table 9). In this solvate, two Li ions are threefold coordinated by three oxygen atoms from two diglyme molecules, evidencing strong interactions with the solvent molecules. It is noteworthy that upon reaching the decomposition temperature, the solid sample starts melting and bubbling. Hydrogen loss from the boron cages was confirmed by ^{1}H NMR and ^{11}B NMR [Supplementary Figures 18-20], as the characteristic asymmetric multiplet of $B_{12}H_{12}^{2-}$ (1.6-0 ppm) disappears after thermal treatment at 170 °C under vacuum for 12 h, indicating competition between desolvation and dehydrogenation[66]. These results suggest that direct removal of diglyme by thermal treatment is not possible.

We investigated a new way to obtain anhydrous $Li_2B_{12}H_{12}$ from glyme solvates, eliminating the need for the previously used and inconvenient ion exchange strategy, by using DMSO or *N*, *N*-diethylformamide (DEF) as solvent exchange agents. This approach aims to overcome the strong chelation of diglyme with dodecaborate salts containing small cations such as Li^+ and Na^+. The methodology consists of adding 10 mL of DMSO or DEF to 1 g of the diglyme-solvated product, followed by drying the solution under vacuum at 100 °C for 12 h. Upon this treatment, completely exchanged DMSO- or DEF-solvated $Li_2B_{12}H_{12}$ is achieved, as demonstrated by powder X-ray diffraction (PXRD) and Fourier transform infrared (FTIR) spectroscopy [Figure 3A-C and Supplementary Figures 21-23]. The ^{1}H NMR analysis [Supplementary Figure 24] of $Li_2B_{12}H_{12}$·n DMSO before and after desolvation indicates that DMSO completely replaces diglyme. Additionally, DMSO can be removed from the solvate by thermal treatment without decomposition of the $B_{12}H_{12}^{2-}$ anion. This suggests that DMSO can be used as an effective solvent for the removal of diglyme in $Li_2B_{12}H_{12}$. Subsequently, drying the solvent-exchanged products at 200 °C under vacuum results in the formation of unsolvated $Li_2B_{12}H_{12}$, as shown by *in situ* PXRD [Supplementary Figure 23] and NMR [Supplementary Figures 24-26]. The choice of DMSO and DEF for solvent exchange is justified by their higher boiling points and weaker coordinating ability compared to diglyme[67]. Although both solvents can effectively substitute diglyme, DMSO is the more economically viable option given the much higher cost of DEF.

When monoglyme is used in the synthesis, the crystalline phase of the obtained solvate corresponds to $Li_2B_{12}H_{12}$·1.5 monoglyme, as evidenced by its structure determined by SC-XRD [Figure 3D, Supplementary Figure 60, Supplementary Table 10]. In this structure, monoglyme shows a coordinating ability toward Li^+ similar to that of diglyme in solvated $Li_2B_{12}H_{12}$, and thus may pose similar challenges for desolvation. However, *in situ* PXRD data [Supplementary Figure 27] reveal that monoglyme-solvated $Li_2B_{12}H_{12}$ undergoes different phase changes during thermal desolvation compared to diglyme-solvated $Li_2B_{12}H_{12}$, ultimately yielding $Li_2B_{12}H_{12}$. Diffraction peaks of the monoglyme-solvated $Li_2B_{12}H_{12}$ disappear at around 150 °C, while $Li_2B_{12}H_{12}$ forms at this temperature. At 310 °C, a phase transition from the α-$Li_2B_{12}H_{12}$ to β-$Li_2B_{12}H_{12}$ is observed, followed by decomposition into a hydrogen-poor γ-$Li_2B_{12}H_{12-x}$ phase at higher temperatures[68,69]. This last phase transition occurs at a temperature approximately 50 °C lower than previously reported, likely due to the experiment being performed under vacuum. An attempt to directly remove monoglyme from the solvated $Li_2B_{12}H_{12}$ by heating at 180 °C under vacuum for 12 h resulted in a small amount of $Li_2B_{12}H_{12-x}$, as observed in the ^{11}B NMR spectrum [Supplementary Figure 28].

Although complete removal of monoglyme from $Li_2B_{12}H_{12}$ through direct heating is difficult, the solvent exchange strategy can in this case be implemented with an even lighter, more abundant, and greener solvent, namely water (H_2O), compared to DMSO and DEF used for the diglyme-solvated dodecaborate. Indeed, upon exchange with water and applying vacuum at 40 °C, monoglyme can be completely removed, as shown in Figure 3D-F and ^{1}H NMR spectra [Supplementary Figures 29-31], and pure hydrated $Li_2B_{12}H_{12}$ can be obtained. Water can then be easily removed from hydrated $Li_2B_{12}H_{12}$ without damaging the $B_{12}H_{12}^{2-}$ clusters.

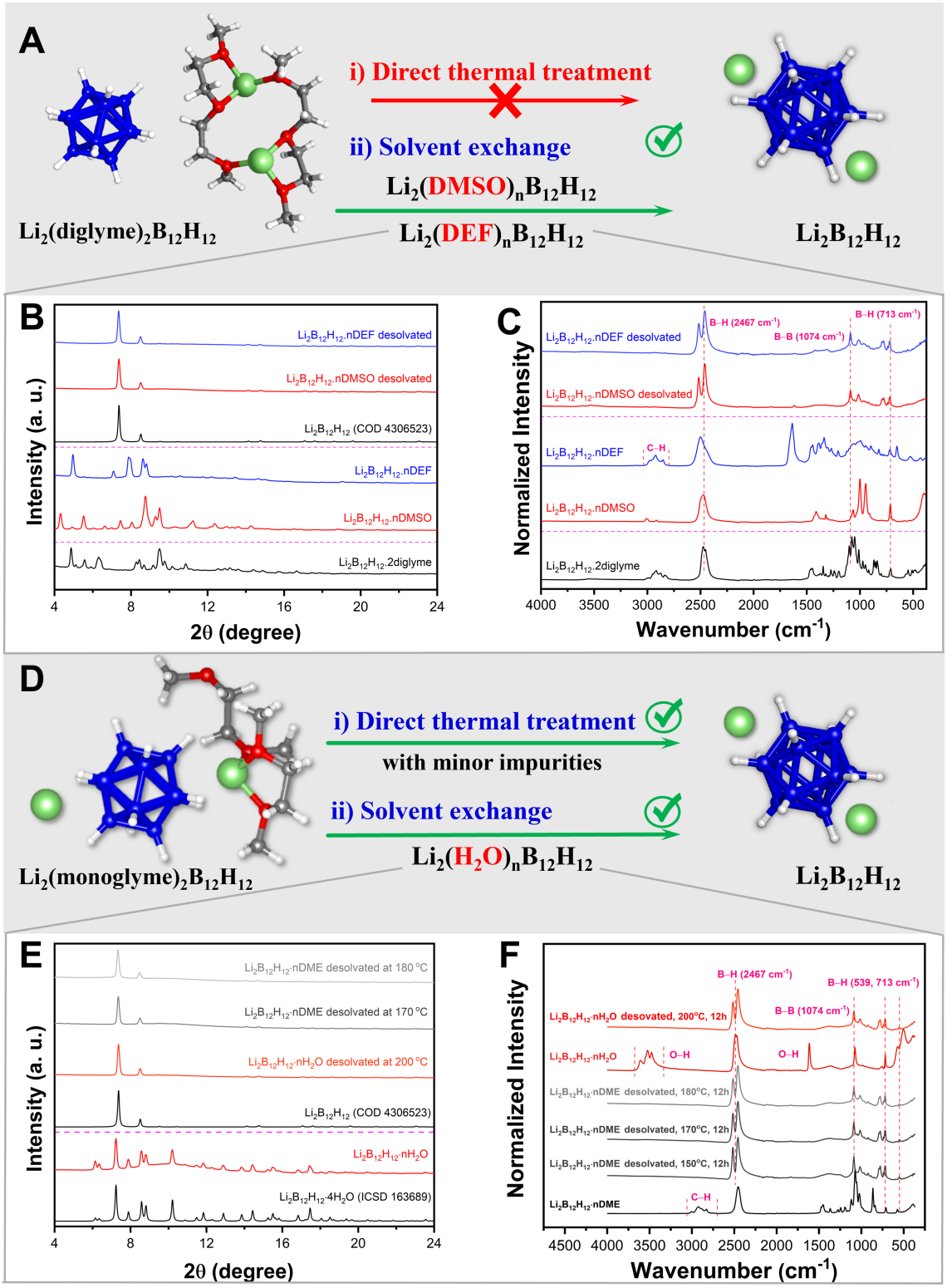

Figure 3. (A) Crystal structure fragment of $Li_2B_{12}H_{12}$·2 diglyme and the approaches used for solvent removal; (B) PXRD (λ = 0.71073 Å) patterns; (C) FTIR spectroscopy spectra of $Li_2B_{12}H_{12}$·n diglyme and DMSO/DEF-substituted samples before and after drying at 200 °C under vacuum; (D) Crystal structure fragment of $Li_2B_{12}H_{12}$·1.5 monoglyme and the approaches used for solvent removal; (E) PXRD patterns (λ = 0.71073 Å); (F) FTIR spectra of $Li_2B_{12}H_{12}$·n DME, $Li_2B_{12}H_{12}$·n H_2O, and anhydrous $Li_2B_{12}H_{12}$ after heat treatment. Color code: Li (green), B (dark blue), H (light grey), O (red), C (dark grey). $Li_2B_{12}H_{12}$: Lithium dodecaborate; PXRD: powder X-ray diffraction; FTIR: Fourier transform infrared; DMSO: dimethyl sulfoxide; DEF: *N*, *N*-diethylformamide; DME: 1,2-dimethoxyethane.

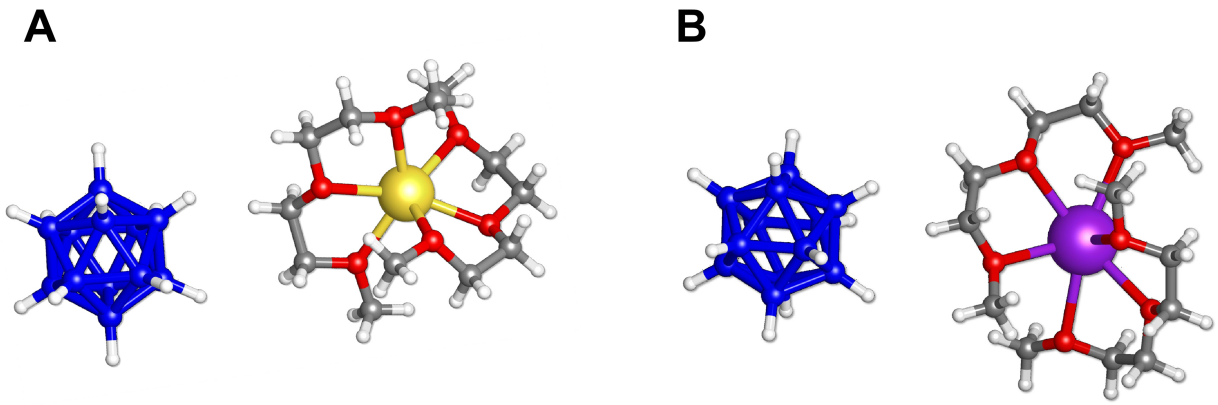

Figure 4. Fragments of the single-crystal structures of (A) $Na_2B_{12}H_{12}$·4 diglyme (RT) and (B) $K_2B_{12}H_{12}$·4 diglyme, illustrating the coordination modes of diglyme to alkali metal cations. Color code: Na, yellow; K, purple; B, dark blue; H, light grey; O, red; C, dark grey. RT: Room temperature.

It is worth noting that $Li_2B_{12}H_{12}$ is commercially available in hydrated form, which can be conveniently obtained by our solvent exchange strategy without the last heating step.

Single crystals of diglyme-solvated $Na_2B_{12}H_{12}$ and $K_2B_{12}H_{12}$ were also isolated from the reaction mixtures during synthesis, and their structures were determined by SC-XRD to be $Na_2B_{12}H_{12}$·4 diglyme [Figure 4A, Supplementary Figure 61, Supplementary Table 10] and $K_2B_{12}H_{12}$·4 diglyme [Figure 4B, Supplementary Figure 62, Supplementary Table 11]. Unlike Li^+, Na^+ and K^+ possess lower charge densities and larger cation sizes, resulting in higher cation-to-anion size ratios[70]. This leads to different coordination environments for Na^+ and K^+, with $M^+\cdots O$ bonds ($Na^+\cdots O$ = 2.378-2.446 Å, $K^+\cdots O$ = 2.728-2.844 Å) longer than $Li^+\cdots O$ = 1.958-2.039 Å, meaning that less energy is needed to break these coordination bonds. This finding explains why direct heat treatment of diglyme-solvated $Na_2B_{12}H_{12}$ (150 °C) and $K_2B_{12}H_{12}$ (200 °C) under vacuum effectively removed diglyme in our previous work, whereas the same approach was ineffective for the Li^+ salt[36].

Interestingly, drying crystals of diglyme-solvated $Na_2B_{12}H_{12}$ at 80 °C for 2 h induced a single-crystal-to-single-crystal transformation, yielding a high-temperature (HT) diglyme-solvated form of $Na_2B_{12}H_{12}$ [Supplementary Figure 63 and Supplementary Table 12]. Decomposition of the HT form, $Na_2B_{12}H_{12}$·2 diglyme, directly yielded anhydrous $Na_2B_{12}H_{12}$ [Supplementary Figures 32-36]. In contrast, decomposition of diglyme-solvated $K_2B_{12}H_{12}$ proceeded steadily in a single step, leading to the formation of $K_2B_{12}H_{12}$, as illustrated in Supplementary Figures 37 and 38.

We also attempted synthesis in toluene, a non-coordinating solvent, with the aim of directly obtaining unsolvated $M_2B_{12}H_{12}$ (M = Li, Na). The ^{11}B NMR spectra [Supplementary Figures 39-41] confirmed the formation of $Li_2B_{12}H_{12}$ along with BH_4^-, $B_{11}H_{14}^-$, $B_{11}H_{13}^{2-}$, and the thiomethyl-substituted cluster $B_{12}H_{11}S(CH_3)^-$[71]. PXRD analysis [Supplementary Figures 42-44] revealed $Li_2B_{12}H_{12}$ as the only crystalline phase when the reaction was performed at 100 °C, while additional impurity peaks appeared at 120 °C. Performing the reaction in an autoclave at 120 °C achieved complete conversion of BH_4^- to $B_{12}H_{12}^{2-}$. We also ball-milled $LiBH_4$ prior to synthesis in toluene to further improve the contact surface, as this reactant is insoluble in the solvent. This pretreatment significantly enhanced its reactivity, leading to the formation of BH_4^- and $B_{11}H_{13}^{2-}$ together with $B_{12}H_{12}^{2-}$ [Supplementary Figures 45-50]. While high-purity $Li_2B_{12}H_{12}$ could be obtained from toluene, post-synthetic solvent extraction was necessary to remove residual byproducts. In contrast, replacing $LiBH_4$ with $NaBH_4$ primarily yielded $NaB_{12}H_{11}S(CH_3)_2$ rather than $Na_2B_{12}H_{12}$

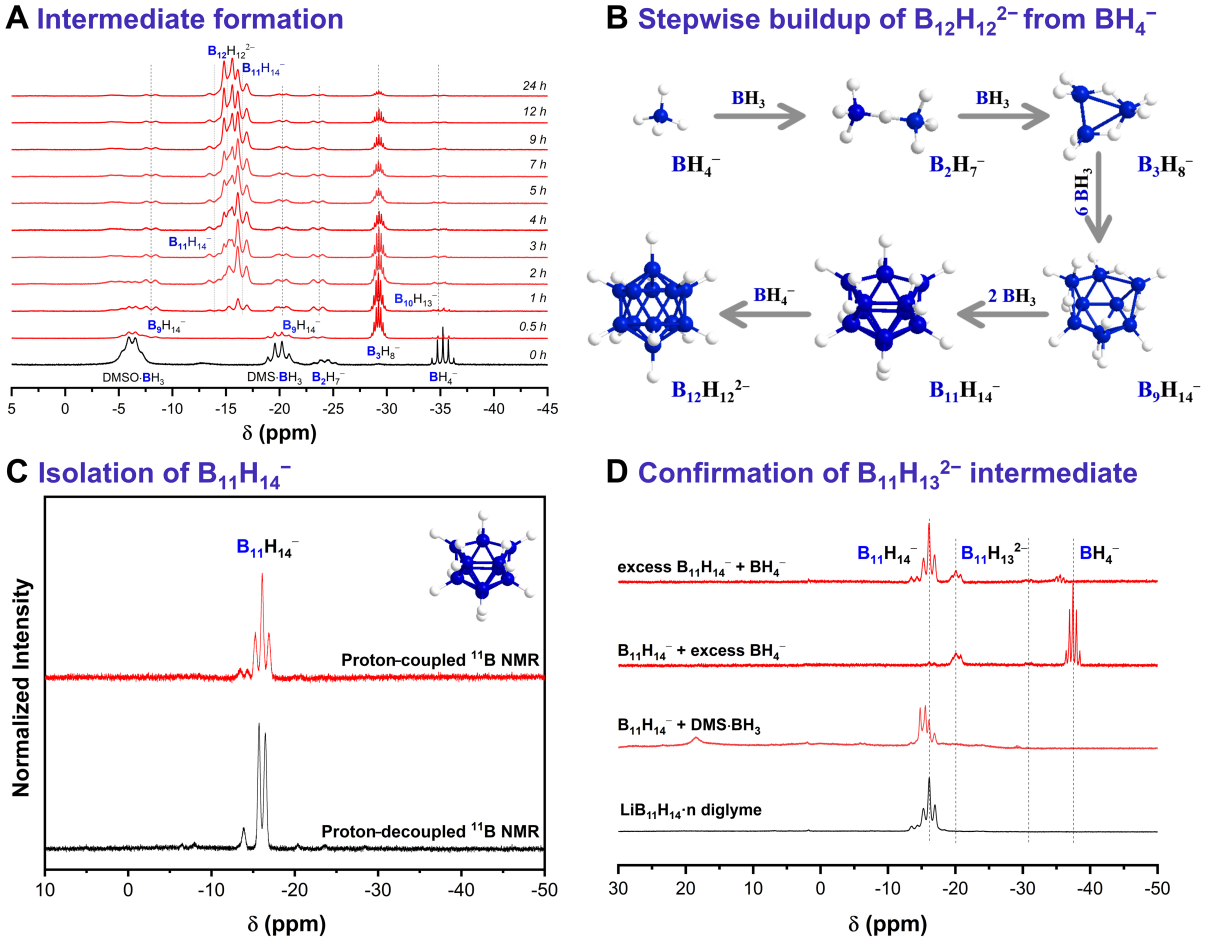

Figure 5. (A) Proton-coupled ^{11}B NMR spectra of aliquots taken from a reaction mixture containing $LiBH_4$ and DMS·BH_3 in diglyme at 120 °C at different time intervals (t = 0 h was sampled before heating the mixture; intensities were normalized to the most intense signal); (B) Proposed sequence for the stepwise formation of $B_{12}H_{12}^{2-}$ from BH_4^-; (C) Proton-decoupled (black) and -coupled (red) ^{11}B NMR spectra of the diethyl ether layer after liquid–liquid extraction of an aqueous solution of diglyme-solvated $Li_2B_{12}H_{12}$; (D) Proton-coupled ^{11}B NMR spectra of reaction mixtures containing $LiB_{11}H_{14}$ and either DMS·BH_3 or $LiBH_4$ in diglyme. ^{11}B NMR: ^{11}B nuclear magnetic resonance; $LiBH_4$: lithium borohydride; DMS·BH_3: borane dimethyl sulfide complex; $Li_2B_{12}H_{12}$: lithium dodecaborate.

[Supplementary Figures 51 and 52]. These results suggest that the coordination and polarization characteristics of the metal cation play critical roles in directing *closo*-borate formation, particularly under conditions where the borohydride precursor exhibits limited solubility in the reaction medium.

Elucidation of the formation mechanism of $B_{12}H_{12}^{2-}$

To gain insight into the mechanism of $B_{12}H_{12}^{2-}$ formation, ^{11}B NMR spectroscopy was employed to monitor the composition of the reaction mixture throughout the synthesis. Figure 5A shows the ^{11}B NMR spectra of aliquots collected from a mixture of $LiBH_4$ and DMS·BH_3 in diglyme before heating (0 h) and at different time points during the solvothermal reaction at 120 °C.

In the initial mixture at room temperature, a signal at -24 ppm was observed together with those of the reactants and was assigned to $B_2H_7^-$[42]. This intermediate was then quickly converted into $B_3H_8^-$, together with $B_9H_{14}^-$, during the first half hour of the solvothermal reaction, in agreement with previous observations[42]. Notably, the intensities of the BH_4^- and DMS·BH_3 signals decreased rapidly after initiating heating, accompanied by increasing concentration of $B_9H_{14}^-$ and $B_{11}H_{14}^-$ during the first hour of the reaction. This

behavior is consistent with earlier reports on the dehydrocondensation of $B_3H_8^-$ with B_2H_6[72]. Furthermore, the characteristic doublet of $B_{12}H_{12}^{2-}$ appeared after only 2 h of reaction, and its intensity increased continuously as the reaction progressed. In contrast, the intensities of the $B_9H_{14}^-$ and $B_{11}H_{14}^-$ signals remained almost constant throughout the reaction, while gradual consumption of $B_3H_8^-$ was observed. The sustained concentrations of $B_9H_{14}^-$ and $B_{11}H_{14}^-$ may indicate that these species act as intermediates in a dynamic equilibrium. Alternatively, their behavior could reflect a kinetic steady state in which the rates of formation and consumption are closely balanced, thereby preventing accumulation despite continuous turnover. Based on these ^{11}B NMR observations, Figure 5B proposes a stepwise formation pathway for $B_{12}H_{12}^{2-}$ involving the key intermediates $B_2H_7^-$, $B_3H_8^-$, $B_9H_{14}^-$, and $B_{11}H_{14}^-$.

The above experiment demonstrates that $B_3H_8^-$, $B_9H_{14}^-$, and $B_{11}H_{14}^-$ are stable intermediates in the sequential buildup of $B_{12}H_{12}^{2-}$ from BH_4^- and BH_3. To understand the final step in the formation mechanism of $Li_2B_{12}H_{12}$, isolation of the intermediate $B_{11}H_{14}^-$ was critical. After several attempts [Supplementary Figures 53-55], this intermediate was successfully isolated by subjecting the reaction filtrate obtained from the initial synthetic step to thermal treatment at 160 °C [Figure 5C, Supplementary Figures 56 and 57]. To identify which species react with $B_{11}H_{14}^-$ to form dodecaborate, a solution of isolated $LiB_{11}H_{14}$ in diglyme was reacted with various lower boranes, including DMS·BH_3 and BH_4^-, at 120 °C in a Schlenk flask for 3 h. As shown in Figure 5D and Supplementary Figure 58, direct reaction of $LiB_{11}H_{14}$ with BH_4^- did not yield $B_{12}H_{12}^{2-}$; instead, it produced $B_{11}H_{13}^{2-}$ through deprotonation of $B_{11}H_{14}^-$ by BH_4^-. On the other hand, reaction of $B_{11}H_{14}^-$ with DMS·BH_3 successfully generated $B_{12}H_{12}^{2-}$, whereas thermal decomposition of DMS·BH_3 under the same conditions did not produce detectable amounts of $B_{12}H_{12}^{2-}$ [Supplementary Figure 58]. Previous reports have demonstrated the isolation of the $B_{12}H_{12}^{2-}$ anion through similar reactions, such as that between $B_{11}H_{14}^-$ and triethylamine borane at 150 °C. It has also been reported that $Na_2B_{12}H_{12}$ can be obtained by reacting $NaB_{11}H_{14}$ with $NaBH_4$ in boiling diglyme (boiling point = 162 °C)[8,37,39,41,55,73]. Our results indicate that at the lower reaction temperature of 120 °C, deprotonation is likely favored over direct hydroboration. Therefore, we propose that $B_{11}H_{13}^{2-}$ serves as the terminal intermediate in this sequential pathway, and that its conversion to $B_{12}H_{12}^{2-}$ proceeds only in the presence of sufficient BH_3.

CONCLUSIONS

This work aims to develop a simple and efficient synthetic route to unsolvated $Li_2B_{12}H_{12}$ with high purity and yield. A solvothermal strategy for $Li_2B_{12}H_{12}$ synthesis based on the reaction of $LiBH_4$ with DMS·BH_3 in glymes was established, enabling the efficient synthesis of $Li_2B_{12}H_{12}$ under optimized conditions with a 96% yield. An innovative methodology involving diglyme exchange enables the preparation of chemically pure $Li_2B_{12}H_{12}$. The reaction intermediates formed during $B_{12}H_{12}^{2-}$ synthesis were elucidated *ex situ* using ^{11}B NMR. The results evidenced a stepwise buildup of $B_{12}H_{12}^{2-}$ from BH_4^- through $B_2H_7^-$, $B_3H_8^-$, $B_9H_{14}^-$, and $B_{11}H_{14}^-$ intermediates. The developed synthetic strategy for lithium and other alkali metal *closo*-dodecaborates, applicable to both solvated and unsolvated forms, represents a substantial advancement over previous approaches in terms of yield, purity, and cost-effectiveness. Beyond offering a practical route to $M_2B_{12}H_{12}$ compounds, this work suggests a possible approach for the synthesis of other *closo*-borate materials that have traditionally relied on cation exchange.

DECLARATIONS

Acknowledgments

Dr. Dmitry Chernyshov and Dr. Iurii Dovgaliuk are acknowledged for their help during synchrotron measurements at the SNBL (Swiss-Norwegian Beamline) of the ESRF (European Synchrotron Radiation Facility) in Grenoble. The authors also acknowledge Dr. Igor E. Golub and Prof. Hans Hagemann (University of Geneva) for their meaningful discussions.

Authors' contributions

Conceived and designed the study, conducted the experiments, performed data analysis and curation, prepared the figures, and wrote the original draft: Wang, J.
Contributed to the experimental work, data analysis, data validation, and manuscript revision: Steenhaut, T.
Carried out single crystal X-ray diffraction analysis, structure refinement, and structural data interpretation, and assisted in manuscript review: Robeyns, K.
Supervised the project, provided resources and funding, managed the research activities, and contributed to manuscript editing: Li, H. W.
Conceived the project, supervised the overall research, contributed to data interpretation, secured funding, and revised the manuscript: Filinchuk, Y.

Availability of data and materials

Detailed experimental procedures, characterizations, and supporting results are available from the Supplementary Materials. CCDC 2489735-2489739 contain the supplementary crystallographic data and can be downloaded free of charge from The Cambridge Crystallographic Data Centre *via* www.ccdc.cam.ac.uk/structures.

AI and AI-assisted tools statement

Not applicable.

Financial support and sponsorship

This work was financially supported by the China Scholarship Council (201806930031), the FNRS (PDR T.0169.13, EQP U.N038.13, J.0164.17, CdR J.0073.20, and J.0168.22), and the Communauté Française de Belgique under Grant ARC 18/23-093.

Conflicts of interest

Li, H. W. and Filinchuk, Y. are Guest Editors of the Special Issue "Advanced Materials for Hydrogen and Energy Storage". Li, H. W. and Filinchuk, Y. were not involved in any stage of the editorial process, notably including reviewer selection, manuscript handling, or decision making. The other authors declared that there are no conflicts of interest.

Ethical approval and consent to participate

Not applicable.

Consent for publication

Not applicable.

Copyright

© The Author(s) 2026.

Supplementary Materials

Supplementary Materials

REFERENCES

1. Chen, C.; Chen, Z.; Zhang, M.; et al. Closo-$[B_{12}H_{12}]^{2-}$ derivatives with polar groups as promising building blocks in metal-organic frameworks for gas separation. *ChemSusChem* **2023**, *16*, e202300434. DOI PubMed
2. Yan, Y.; Kühnel, R.; Remhof, A.; et al. A lithium amide-borohydride solid-state electrolyte with lithium-ion conductivities comparable to liquid electrolytes. *Adv. Energy. Mater.* **2017**, *7*, 1700294. DOI
3. Chen, C.; Ding, Z.; Gao, Y.; et al. Recent advances in boron chemistry. *Sci. China. Chem.* **2025**, *68*, 3927-95. DOI
4. Wang, L.; Jiang, Y.; Duttwyler, S.; Lin, F.; Zhang, Y. Chemistry of three-dimensional icosahedral boron clusters anions: closo-dodecaborate (2-) $[B_{12}H_{12}]^{2-}$ and carba-closo-dodecaborate(-) $[CB_{11}H_{12}]^{-}$. *Coord. Chem. Rev.* **2024**, *516*, 215974. DOI
5. Ould, D. M. C.; Menkin, S.; Smith, H. E.; et al. Sodium borates: expanding the electrolyte selection for sodium-ion batteries. *Angew. Chem. Int. Ed. Engl.* **2022**, *61*, e202202133. DOI PubMed PMC

6. Green, M.; Kaydanik, K.; Orozco, M.; et al. Closo-borate gel polymer electrolyte with remarkable electrochemical stability and a wide operating temperature window. *Adv. Sci.* **2022**, *9*, e2106032. DOI PubMed PMC
7. Neumolotov, N. K.; Selivanov, N. A.; Bykov, A. Y.; et al. New methods for preparation of the monofluorosubstituted derivative of the closo-borate anion $[2\text{-}B_{10}H_9F]^{2-}$, its properties, and analysis of its reactivity. *Russ. J. Inorg. Chem.* **2022**, *67*, 1583-90. DOI
8. Adams, R. M.; Siedle, A. R.; Grant, J. Convenient preparation of the dodecahydrododecaborate ion. *Inorg. Chem.* **1964**, *3*, 461. DOI
9. Eberhardt, W. H.; Crawford, B.; Lipscomb, W. N. The valence structure of the boron hydrides. *J. Chem. Phys.* **1954**, *22*, 989-1001. DOI
10. Pitochelli, A. R.; Hawthorne, F. M. The isolation of the icosahedral $B_{12}H_{12}^{-2}$ ion. *J. Am. Chem. Soc.* **1960**, *82*, 3228-9. DOI
11. Jin, M.; Xu, D.; Su, Z.; et al. Hydridoborate-based solid electrolytes for all-solid-state batteries. *Adv. Mater.* **2025**, e07809. DOI PubMed
12. Paskevicius, M.; Jepsen, L. H.; Schouwink, P.; et al. Metal borohydrides and derivatives - synthesis, structure and properties. *Chem. Soc. Rev.* **2017**, *46*, 1565-634. DOI PubMed
13. Bukovsky, E. V.; Peryshkov, D. V.; Wu, H.; et al. Comparison of the coordination of $B_{12}F_{12}^{2-}$, $B_{12}Cl_{12}^{2-}$, and $B_{12}H_{12}^{2-}$ to Na^+ in the solid state: crystal structures and thermal behavior of $Na_2(B_{12}F_{12})$, $Na_2(H_2O)_4(B_{12}F_{12})$, $Na_2(B_{12}Cl_{12})$, and $Na_2(H_2O)_6(B_{12}Cl_{12})$. *Inorg. Chem.* **2017**, *56*, 4369-79. DOI PubMed
14. Campos dos Santos, E.; Sato, R.; Kisu, K.; et al. Explore the ionic conductivity trends on $B_{12}H_{12}$ divalent *Closo*-type complex hydride electrolytes. *Chem. Mater.* **2023**, *35*, 5996-6004. DOI
15. Zhou, C.; Yan, Y.; Jensen, T. R. Enhanced electrochemical performance of the $Li_2B_{12}H_{12}$-$Li_2B_{10}H_{10}$-$LiBH_4$ electrolyte. *ACS. Appl. Energy. Mater.* **2023**, *6*, 7346-52. DOI
16. Maltsev, A. P.; Chepkasov, I. V.; Oganov, A. R. Order-disorder phase transition and ionic conductivity in a $Li_2B_{12}H_{12}$ solid electrolyte. *ACS. Appl. Mater. Interfaces.* **2023**, *15*, 42511-9. DOI PubMed
17. Simonyan, H.; Zhong, L.; Green, M. M.; et al. Solvation environment and interface dynamics of $Li_2B_{12}H_{12}$ and $Li_2B_{12}F_{12}$ electrolytes uncovered by theory and operando optical and FTIR spectroelectrochemistry. *ACS. Appl. Mater. Interfaces.* **2024**, *16*, 70028-37. DOI PubMed PMC
18. Asakura, R.; Łodziana, Z.; Grissa, R.; Rentsch, D.; Battaglia, C.; Remhof, A. Unveiling solid-state electrochemical oxidation of $LiBH_4$ and $Li_2B_{12}H_{12}$ for high-voltage all-solid-state batteries. *ACS. Appl. Energy. Mater.* **2025**, *8*, 9637-45. DOI
19. Zhou, C.; Grinderslev, J. B.; Skov, L. N.; et al. Polymorphism, ionic conductivity and electrochemical properties of lithium *closo*-deca- and dodeca-borates and their composites, $Li_2B_{10}H_{10}$–$Li_2B_{12}H_{12}$. *J. Mater. Chem. A.* **2022**, *10*, 16137-51. DOI
20. Pang, Y.; Liu, Y.; Yang, J.; Zheng, S.; Wang, C. Hydrides for solid-state batteries: a review. *Mater. Today. Nano.* **2022**, *18*, 100194. DOI
21. Grams, R. J.; Santos, W. L.; Scorei, I. R.; et al. The rise of boron-containing compounds: advancements in synthesis, medicinal chemistry, and emerging pharmacology. *Chem. Rev.* **2024**, *124*, 2441-511. DOI PubMed
22. Bachman, J. C.; Muy, S.; Grimaud, A.; et al. Inorganic solid-state electrolytes for lithium batteries: mechanisms and properties governing ion conduction. *Chem. Rev.* **2016**, *116*, 140-62. DOI PubMed
23. Barth, R. F.; Mi, P.; Yang, W. Boron delivery agents for neutron capture therapy of cancer. *Cancer. Commun.* **2018**, *38*, 35. DOI PubMed PMC
24. He, Z.; Xiong, J.; Zuo, Y.; et al. Efficient targeted regulation of the interfaces and bulk in inverted perovskite solar cells with a [*closo*-$B_{12}H_{12}$]$^{2-}$-based derivative. *Adv. Mater.* **2025**, *37*, e2414155. DOI PubMed
25. Huang, Z.; Wang, S.; Dewhurst, R. D.; Ignat'ev, N. V.; Finze, M.; Braunschweig, H. Boron: its role in energy-related processes and applications. *Angew. Chem. Int. Ed. Engl.* **2020**, *59*, 8800-16. DOI PubMed PMC
26. Li, J.; Kim, J. S.; Fan, J.; Peng, X.; Matějíček, P. Boron cluster leveraged polymeric building blocks. *Chem. Soc. Rev.* **2025**, *54*, 4104-34. DOI PubMed
27. Xu, X.; Deng, X.; Li, Y.; et al. Applications of boron cluster supramolecular frameworks as metal-free chemodynamic therapy agents for melanoma. *Small* **2024**, *20*, e2307029. DOI PubMed
28. Sivaev, I. B.; Prikaznov, A. V.; Naoufal, D. Fifty years of the closo-decaborate anion chemistry. *Collect. Czech. Chem. Commun.* **2010**, *75*, 1149-99. DOI
29. Miller, H. C.; Miller, N. E.; Muetterties, E. L. Synthesis of polyhedral boranes. *J. Am. Chem. Soc.* **1963**, *85*, 3885-6. DOI
30. Hansen, B. R. S.; Paskevicius, M.; Li, H. W.; Akiba, E.; Jensen, T. R. Metal boranes: progress and applications. *Coord. Chem. Rev.* **2016**, *323*, 60-70. DOI
31. Chen, W.; Wu, G.; He, T.; et al. An improved synthesis of unsolvated NaB_3H_8 and its application in preparing $Na_2B_{12}H_{12}$. *Int. J. Hydrogen. Energy.* **2016**, *41*, 15471-6. DOI

32. Moury, R.; Gigante, A.; Hagemann, H. An alternative approach to the synthesis of NaB_3H_8 and $Na_2B_{12}H_{12}$ for solid electrolyte applications. *Int. J. Hydrogen. Energy.* **2017**, *42*, 22417-21. DOI
33. He, L.; Li, H.; Hwang, S. J.; Akiba, E. Facile solvent-free synthesis of anhydrous alkali metal dodecaborate $M_2B_{12}H_{12}$ (M = Li, Na, K). *J. Phys. Chem. C.* **2014**, *118*, 6084-9. DOI
34. Remhof, A.; Yan, Y.; Rentsch, D.; Borgschulte, A.; Jensen, C. M.; Züttel, A. Solvent-free synthesis and stability of $MgB_{12}H_{12}$. *J. Mater. Chem. A.* **2014**, *2*, 7244-9. DOI
35. Yan, Y.; Rentsch, D.; Battaglia, C.; Remhof, A. Synthesis, stability and Li-ion mobility of nanoconfined $Li_2B_{12}H_{12}$. *Dalton. Trans.* **2017**, *46*, 12434-7. DOI PubMed
36. Wang, J.; Steenhaut, T.; Li, H. W.; Filinchuk, Y. High yield autoclave synthesis of pure $M_2B_{12}H_{12}$ (M = Na, K). *Inorg. Chem.* **2023**, *62*, 2153-60. DOI PubMed
37. Jing, Y.; Wang, X.; Han, H.; et al. Selective synthesis of the $B_{11}H_{14}^-$ and $B_{12}H_{12}^{2-}$ borane derivatives and the general mechanisms of the B-H bond condensation. *Sci. China. Chem.* **2024**, *67*, 876-81. DOI
38. Han, H.; Liu, X. R.; Gao, Y. M.; et al. An improved method for the synthesis of $M_2[B_{12}H_{12}]$ (M = Na, K) and their formation mechanism. *Inorg. Chem.* **2024**, *63*, 13886-92. DOI PubMed
39. Jing, Y.; Liu, X. R.; Wang, X.; et al. Facile synthesis of the dodecahydridododecaborate ($B_{12}H_{12}^{2-}$) from borane Lewis base adducts. *Sci. China. Chem.* **2025**, *68*, 1355-61. DOI
40. Zhou, C.; Sun, H.; Wang, Q.; et al. Highly electrochemically stable $Li_2B_{12}H_{12}$-Al_2O_3 nanocomposite electrolyte enabling A 3.8 V room-temperature all-solid-state Li-ion battery. *J. Alloys. Compd.* **2023**, *938*, 168689. DOI
41. Souza, D. H. P.; Møller, K. T.; Moggach, S. A.; et al. Hydrated alkali-$B_{11}H_{14}$ salts as potential solid-state electrolytes. *J. Mater. Chem. A.* **2021**, *9*, 15027-37. DOI
42. Chen, X. M.; Ma, N.; Zhang, Q. F.; et al. Elucidation of the formation mechanisms of the octahydrotriborate anion ($B_3H_8^-$) through the nucleophilicity of the B-H bond. *J. Am. Chem. Soc.* **2018**, *140*, 6718-26. DOI PubMed
43. Huang, Z.; Gallucci, J.; Chen, X.; et al. $Li_2B_{12}H_{12}$·$7NH_3$: a new ammine complex for ammonia storage or indirect hydrogen storage. *J. Mater. Chem.* **2010**, *20*, 2743-5. DOI
44. Kisu, K.; Kim, S.; Shinohara, T.; Zhao, K.; Züttel, A.; Orimo, S. I. Monocarborane cluster as a stable fluorine-free calcium battery electrolyte. *Sci. Rep.* **2021**, *11*, 7563. DOI PubMed PMC
45. Johnson, S. I.; Demaria, J. M.; Ginovska, B.; Edvenson, G. M.; Hagemann, H.; Autrey, S. T. Exploring detailed reaction pathways for hydrogen storage with borohydrides using DFT calculations. *Energy. Fuels.* **2022**, *36*, 5513-27. DOI
46. Pitt, M. P.; Paskevicius, M.; Brown, D. H.; Sheppard, D. A.; Buckley, C. E. Thermal stability of $Li_2B_{12}H_{12}$ and its role in the decomposition of $LiBH_4$. *J. Am. Chem. Soc.* **2013**, *135*, 6930-41. DOI PubMed
47. Yan, Y.; Remhof, A.; Rentsch, D.; Züttel, A. The role of $MgB_{12}H_{12}$ in the hydrogen desorption process of $Mg(BH_4)_2$. *Chem. Commun.* **2015**, *51*, 700-2. DOI PubMed
48. Sethio, D.; Daku, L. M. L.; Hagemann, H.; Kraka, E. Quantitative assessment of B-B-B, B-H_b-B, and B-H_t bonds: from BH_3 to $B_{12}H_{12}^{2-}$. *Chemphyschem* **2019**, *20*, 1967-77. DOI PubMed
49. Bhattacharyya, P.; Boustani, I.; Shukla, A. Why does a $B_{12}H_{12}$ icosahedron need two electrons to be stable: a first-principles electron-correlated investigation of $B_{12}H_n$ (n = 6, 12) clusters. *J. Phys. Chem. A.* **2021**, *125*, 10734-41. DOI PubMed
50. Chen, X.; Liu, X. R.; Wang, X.; Chen, X. M.; Jing, Y.; Wei, D. A safe and efficient synthetic method for alkali metal octahydrotriborates, unravelling a general mechanism for constructing the delta B3 unit of polyhedral boranes. *Dalton. Trans.* **2021**, *50*, 13676-9. DOI PubMed
51. Zhao, Q.; Dewhurst, R. D.; Braunschweig, H.; Chen, X. A new perspective on borane chemistry: the nucleophilicity of the B-H bonding pair electrons. *Angew. Chem. Int. Ed. Engl.* **2019**, *58*, 3268-78. DOI PubMed
52. Avdeeva, V. V.; Malinina, E. A.; Sivaev, I. B.; Bregadze, V. I.; Kuznetsov, N. T. Silver and copper complexes with *closo*-polyhedral borane, carborane and metallacarborane anions: synthesis and X-ray structure. *Crystals* **2016**, *6*, 60. DOI
53. Ďorďovič, V.; Tošner, Z.; Uchman, M.; et al. Stealth amphiphiles: self-assembly of polyhedral boron clusters. *Langmuir* **2016**, *32*, 6713-22. DOI PubMed
54. Dunks, G. B.; Barker, K.; Hedaya, E.; Hefner, C.; Palmer-Ordonez, K.; Remec, P. Simplified synthesis of decaborane(14) from sodium tetrahydroborate via tetradecahydroundecaborate(1-) ion. *Inorg. Chem.* **1981**, *20*, 1692-7. DOI
55. Yin, Y.; Yan, F.; Li, S.; et al. Nature-inspired strategy: novel borohydride-based solid electrolytes extracted from cathode-electrolyte interphase. *Adv. Mater.* **2024**, *36*, e2406632. DOI PubMed

56. Siedle, A. R.; Bodner, G. M.; Todd, L. J. Studies in boron hydrides - V: assignment of the ^{11}B NMR spectrum of the tridecahydro decaborate(1-) ion. *J. Inorg. Nucl. Chem.* **1971**, *33*, 3671-6. DOI
57. Kultyshev, R. G.; Liu, J.; Meyers, E. A.; Shore, S. G. Synthesis and characterization of sulfide, sulfide-sulfonium, and bissulfide derivatives of $[B_{12}H_{12}]^{2-}$. Additivity of Me_2S and MeS^- substituent effects in ^{11}B NMR spectra of disubstituted icosahedral boron clusters. *Inorg. Chem.* **2000**, *39*, 3333-41. DOI PubMed
58. Gigante, A.; Duchêne, L.; Moury, R.; Pupier, M.; Remhof, A.; Hagemann, H. Direct solution-based synthesis of $Na_4(B_{12}H_{12})(B_{10}H_{10})$ solid electrolyte. *ChemSusChem* **2019**, *12*, 4832-7. DOI PubMed
59. Fu, H.; Wang, X.; Shao, Y.; et al. Synthesis of lithium octahydrotriborate and investigation on its thermal decomposition. *Int. J. Hydrogen. Energy.* **2016**, *41*, 384-91. DOI
60. Chen, X. M.; Jing, Y.; Kang, J. X.; et al. Synthesis, formation mechanism, and structure of $K[BH_3S(CH_3)BH_3]$ and its application in preparation of KB_3H_8. *Inorg. Chem.* **2022**, *61*, 12828-34. DOI PubMed
61. Mishchenko, A. M.; Nechayev, M. A.; Subota, A. I.; et al. A new convenient method for preparing tetrabutylammonium closo-dodecaborate. *J. Org. Pharm. Chem.* **2024**, *22*, 3-9. DOI
62. Zheng, X.; Yang, Y.; Zhao, F.; Fang, F.; Guo, Y. Facile preparation and dehydrogenation of unsolvated KB_3H_8. *Chem. Commun.* **2017**, *53*, 11083-6. DOI PubMed
63. Hwang, S. J.; Bowman, R. C.; Reiter, J. W.; et al. NMR confirmation for formation of $[B_{12}H_{12}]^{2-}$ complexes during hydrogen desorption from metal borohydrides. *J. Phys. Chem. C.* **2008**, *112*, 3164-9. DOI
64. Chen, X. M.; Ma, N.; Liu, X. R.; et al. Facile synthesis of unsolvated alkali metal octahydrotriborate salts MB_3H_8 (M=K, Rb, and Cs), mechanisms of formation, and the crystal structure of KB_3H_8. *Angew. Chem. Int. Ed. Engl.* **2019**, *58*, 2720-4. DOI PubMed
65. Kotlensky, W. V.; Schaeffer, R. Decomposition of diborane in a silent discharge. Isolation of B_6H_{10} and B_9H_{15}. *J. Am. Chem. Soc.* **1958**, *80*, 4517-9. DOI
66. Chen, X.; Liu, Y. H.; Alexander, A. M.; et al. Desolvation and dehydrogenation of solvated magnesium salts of dodecahydrododecaborate: relationship between structure and thermal decomposition. *Chemistry* **2014**, *20*, 7325-33. DOI PubMed
67. Alvarez, S. Coordinating ability of anions, solvents, amino acids, and gases towards alkaline and alkaline-earth elements, transition metals, and lanthanides. *Chemistry* **2020**, *26*, 4350-77. DOI PubMed
68. Paskevicius, M.; Pitt, M. P.; Brown, D. H.; Sheppard, D. A.; Chumphongphan, S.; Buckley, C. E. First-order phase transition in the $Li_2B_{12}H_{12}$ system. *Phys. Chem. Chem. Phys.* **2013**, *15*, 15825-8. DOI PubMed
69. Yan, Y.; Wang, H.; Zhu, M.; Cai, W.; Rentsch, D.; Remhof, A. Direct rehydrogenation of $LiBH_4$ from H-deficient $Li_2B_{12}H_{12-x}$. *Crystals* **2018**, *8*, 131. DOI
70. Payandeh, S.; Rentsch, D.; Łodziana, Z.; et al. *Nido*-hydroborate-based electrolytes for all-solid-state lithium batteries. *Adv. Funct. Mater.* **2021**, *31*, 2010046. DOI
71. Hamilton, E. J. M.; Jordan; Meyers, E. A.; Shore, S. G. One-step preparation of dimethyl sulfide substituted icosahedral boranes: the crystal and molecular structures of 1,7-$(SMe_2)_2B_{12}H_{10}$, 1,12-$(SMe_2)_2B_{12}H_{10}$, and $[SMe_3][B_{12}H_{11}(SMe_2)]$·MeCN. *Inorg. Chem.* **1996**, *35*, 5335-41. DOI
72. Gavrilova, L. A.; Titov, L. V.; Petrovskii, P. V. Synthesis of $Bu_4NB_{11}H_{14}$ by the reaction of tetrabutylammonium octahydrotriborate with diborane in diglyme. *Russ. J. Coord. Chem.* **2004**, *30*, 307-8. DOI
73. Volkov, O.; Paetzold, P. The chemistry of the undecaborates. *J. Organomet. Chem.* **2003**, *680*, 301-11. DOI

Disclaimer/Publisher's Note: All statements, opinions, and data contained in this publication are solely those of the individual author(s) and contributor(s) and do not necessarily reflect those of OAE and/or the editor(s). OAE and/or the editor(s) disclaim any responsibility for harm to persons or property resulting from the use of any ideas, methods, instructions, or products mentioned in the content.

© The Author(s) 2026. Open Access This article is licensed under a Creative Commons Attribution 4.0 International License (https://creativecommons.org/licenses/by/4.0/), which permits unrestricted use, sharing, adaptation, distribution and reproduction in any medium or format, for any purpose, even commercially, as long as you give appropriate credit to the original author(s) and the source, provide a link to the Creative Commons license, and indicate if changes were made.

Jian Wang

Dr. Jian Wang obtained his B.Sc. degree in chemistry from the Wuhan Institute of Technology in 2015 and his M.Sc. degree in chemistry from Taiyuan University of Technology in 2018. He received his Ph.D. degree from Université catholique de Louvain in 2024 under the supervision of Prof. Yaroslav Filinchuk. He is currently a postdoctoral researcher in Prof. Hai-Wen Li's group at the School of Advanced Energy, Sun Yat-sen University. His research interests include solid-state hydrogen storage, hydride-based solid electrolytes, and functional materials for energy applications.

Timothy Steenhaut

Dr. Timothy Steenhaut is currently a postdoctoral researcher in quantum materials discovery at the University of Copenhagen, Denmark. He obtained his PhD at UCLouvain (Belgium) in 2022, where he focused on the synthesis and characterization of heterometallic and functionalized metal–organic frameworks (MOFs). He subsequently conducted postdoctoral research on solid-state electrolytes and hydrogen storage in porous materials. His expertise includes advanced materials synthesis, gas sorption, and structural characterization using (in situ) powder diffraction and total scattering techniques, notably pair distribution function (PDF) analysis. He has extensive experience with large-scale facilities, including synchrotron and neutron sources. His research addresses synthesis-structure-property relationships in crystalline, disordered, and nanostructured materials for energy- and materials-related applications.

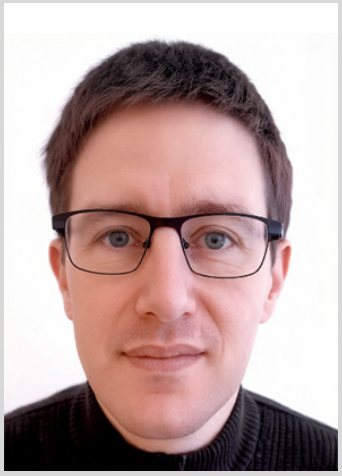

Koen Robeyns

Dr. Koen Robeyns received his Ph.D. degree in chemistry from KU Leuven, Belgium, in 2006. He then worked at the Department of Chemistry, KU Leuven, from 2003 to 2010, focusing on X-ray crystallography and structural analysis. Since 2010, he has been a research engineer at the Institute of Condensed Matter and Nanosciences, Université catholique de Louvain, where he is responsible for X-ray diffraction facilities and structural characterization of crystalline materials. His research interests include X-ray crystallography, crystal structure determination, and the structural chemistry of functional materials.

Hai-Wen Li

Dr. Hai-Wen Li is a tenured Full Professor at the School of Advanced Energy, Sun Yat-sen University (Shenzhen Campus), China. He received his Ph.D. degree in 2005 from the Kitami Institute of Technology, Japan. Following his doctoral training, he carried out research at the Institute for Materials Research, Tohoku University, where he served as a Postdoctoral Researcher, JSPS Postdoctoral Fellow, and Assistant Professor between 2005 and 2011. From 2011 to 2020, Dr. Li was an Associate Professor at the International Research Center for Hydrogen Energy and the International Institute for Carbon-Neutral Energy Research, Kyushu University, Japan. He subsequently served as a Professor at the Hefei General Machinery Research Institute, China, from 2020 to 2024, before joining Sun Yat-sen University. Dr. Li's research interests focus on the design and development of advanced materials and integrated systems for hydrogen, electrochemical, and thermal energy storage.

Yaroslav Filinchuk

Dr. Yaroslav Filinchuk is a Professor at the Institute of Condensed Matter and Nanosciences, Université catholique de Louvain, Belgium. He studied Chemistry at Lviv National University and received a Ph.D in Inorganic Chemistry in 2002. He joined the University of Geneva in 2000, where he began to work on metal hydrides with Prof. Klaus Yvon. In 2006-2010, he worked at the Swiss–Norwegian Beam Lines at the European Synchrotron Radiation Facility. Since 2011, he has been a professor of structural chemistry at the Université catholique de Louvain. His research interests include the chemistry of hydrogen-rich solids, in particular for hydrogen storage, porous materials, and various applications of crystallography in materials science.